

2. M. E. Raichle, *Brain Res. Rev.* 1, 47 (1979); M. E. Raichle *et al.*, *Am. J. Physiol.* 228, 1936 (1975); R. A. Hawkins, W. K. Hass, J. Rausahoff, *Stroke* 10, 690 (1979).
3. L. Sokoloff *et al.*, *J. Neurochem.* 28, 897 (1977); L. Sokoloff, *Brain* 102, 653 (1979); R. C. Collins, J. B. Posner, F. Plum, *Am. J. Physiol.* 218, 943 (1970); S. C. Huang *et al.*, *ibid.* 238, 269 (1980).
4. R. A. Hawkins and A. L. Miller, *Neuroscience* 3, 251 (1978); W. C. Sacks, S. Sacks, A. Fleischer, *Neurochem. Res.* 8, 661 (1983); W. M. Pardridge, *Physiol. Rev.* 63, 1481 (1983).
5. R. S. Balaban, *Am. J. Physiol.* 246, C10 (1984).
6. J. J. H. Ackerman *et al.*, *Nature (London)* 283, 167 (1980); J. L. Evelhoch, M. C. Crowley, J. J. H. Ackerman, *J. Magn. Res.* 56, 110 (1984); R. K. Deuel, *Pediatrics* 70, 650 (1982).
7. Data analysis was carried out after combining the 5-minute collections into 10-minute blocks. Relative concentrations were determined (i) by integrating the area under the peak after convolution difference and resolution enhancement (see Fig. 1); (ii) by measuring the PME peak height (by computer) after removal of baseline artifact by Chebyshev polynomial fit and subtraction [J. J. H. Ackerman *et al.*, *J. Magn. Res.* 56, 318 (1984)]; and (iii) by measuring the PME peak height (manually) relative to the bone phosphorus-derived baseline (Fig. 2A) with β -ATP concentration used as a covariable for each individual animal to compensate statistically for possible minor differences in brain volume observed by the surface coil in different rats. All three methods yielded similar results.
8. Brains were dissected at -20°C , and 50 mg of cerebral cortex was lyophilized, weighed, and treated with trimethylsilylating reagent [A. L. Leavitt and W. R. Sherman, *Methods Enzymol.* 89, 9 (1982)]. Aliquots were separated by gas chromatography on a 4-foot by 0.25-inch column packed with 3 percent OV-17. The effluent was measured with a flame photometric detector operated in the phosphorus-selective mode. Control tissue samples contained small amounts of an uncharacterized phosphorus-containing substance that eluted with the first of the two trimethylsilyl 2-dGlc-6-P peaks; therefore, in all analyses only the second of the 2-dGlc-6-P peaks was used for quantification. In validating the GC analyses, GC-MS was carried out on the same column with ammonia chemical ionization. The substance from the cerebral cortex of rats treated with 2-dGlc had the same protonated molecular ion (m/z , 605) as authentic pentamethylsilyl 2-dGlc-6-P; also, like the authentic material, it eluted from the chromatography column as two peaks, which presumably represent the α and β anomers of 2-dGlc-6-P. Quantitative measurements by GC-MS of three samples at 1.5, 2.5, and 3.5 hours gave results identical with the corresponding data from GC at the flame photometric detector.
9. J. H. Zar, *Biostatistical Analysis* (Prentice-Hall, New York, 1974), p. 228.
10. J. L. Fox, *Science* 224, 143 (1984).
11. T. Nelson, E. E. Kaufman, L. Sokoloff, *J. Neurochem.* 43, 949 (1984).
12. Chemical shifts for both P_i and 2-dGlc-6-P were used independently to measure pH after resolution enhancement by means of curves plotting chemical shift against pH derived in our laboratory [I. A. Bailey *et al.*, *Biochem. J.* 196, 171 (1981)]; both measurements gave the same results.
13. A. Gjedde, *Brain Res. Rev.* 4, 237 (1982); P. D. Crane *et al.*, *J. Neurochem.* 36, 1601 (1981).
14. Rats used in brain histology experiments were managed in the same way as those used for NMR and GC studies except that they were killed at 4, 48, and 92 hours after the bolus injection of 2-dGlc and perfused with saline and formaldehyde. Brains were then cut in 30- μm sections and stained with thionin.
15. Because studies performed in vitro have shown *myo*-inositol-1-phosphate synthase to transform 2-dGlc-6-P to 5-deoxy-*myo*-inositol 1-phosphate and have also shown this substance to be hydrolyzed to 5-deoxy-*myo*-inositol by *myo*-inositol 1-phosphatase (Y.-H. H. Wong and W. R. Sherman, *J. Biol. Chem.*, in press), cerebral cortex was examined for these deoxy-inositols by GC-MS. A lower limit of detectability for the substances under the conditions employed is about 0.1 mmol per kilogram of tissue (wet weight). However, none was found, so this pathway cannot make a significant contribution to the disappearance of 2-dGlc-6-P.
16. J. M. Anchors and M. L. Karnovsky, *J. Biol. Chem.* 250, 6408 (1975); M. Huang and R. L. Veech, *ibid.* 257, 11358 (1982); H. R. Stephens and E. B. Sandborn, *Brain Res.* 113, 127 (1976); M. L. Karnovsky, B. L. Burrows, M. A. Zoccoli in *Cerebral Metabolism and Neural Func-*

tion, J. V. Passoneau, R. A. Hawkins, W. D. Lust, F. A. Walsh, Eds. (Williams and Wilkins, Baltimore, 1980), pp. 359-366; R. W. Horton, B. S. Meldron, H. S. Bachelard, *J. Neurochem.* 21, 507 (1973).

17. Supported by NIH grant GM-30331, NSF grant CHE-8100211, and funding from the McDonnell Center for Study of Higher Brain Functions and the Washington University Mass Spectrometry

Facility (RR-00954, AM-20579). We thank S. Sondgeroth and S. Goodman for adapting the rats; L. Munsell and R. Berger for the GC and GC-MS analyses, respectively; and G. Levy for providing NMR software (National Institutes of Health Biotechnology Research Resource grant RR-01317).

21 September 1984; accepted 4 March 1985

Sonar Tracking of Horizontally Moving Targets by the Big Brown Bat *Eptesicus fuscus*

Abstract. When following a moving target, echolocating bats (*Eptesicus fuscus*) keep their heads aimed at the target's position. This tracking behavior seems not to involve predicting the target's trajectory, but is achieved by the bat's pointing its head at the target's last known position. The bat obtains frequent position updates by emitting sonar signals at a high rate. After the lag between head and target positions and the nonunity tracking gain were corrected for, bats' tracking accuracy in the horizontal plane was $\pm 1.6^{\circ}$.

Most species of echolocating bats are insectivorous and use their sonar system to locate, identify and capture flying insects (1). During pursuit the bat keeps its head aimed at the target as it follows and finally intercepts it. The accuracy of head-aim tracking as measured from stroboscopic photographs of bats maneuvering to catch prey is about $\pm 5^{\circ}$ (2). A bat's capture success depends on knowing the prey's location throughout the interception process. Head-aim tracking keeps prey in front of the bat, where angular acoustic resolution is best, on the order of $\pm 1.5^{\circ}$ as measured with stationary targets (3). In addition, by keeping prey in the middle of the

echolocation sound beam, head tracking functions as one of several gain control mechanisms that reduce variation in the perceived echo strength as the bat closes in on its prey (4).

Bats hunting by sonar do not receive continuous information about target location, but, rather, the echo from each sonar emission provides an acoustic "snapshot" from which the bat updates its current perception of range and position. Through the use of these snapshots, a bat could keep track of prey by two general techniques. It could simply keep its head pointed at the target's last known position (a nonpredictive tracking strategy), or it could attempt to predict the target's trajectory on the basis of the history of target parameters such as position, velocity, and acceleration (a predictive strategy). Since photographic techniques are not sufficiently accurate to distinguish between these two types of

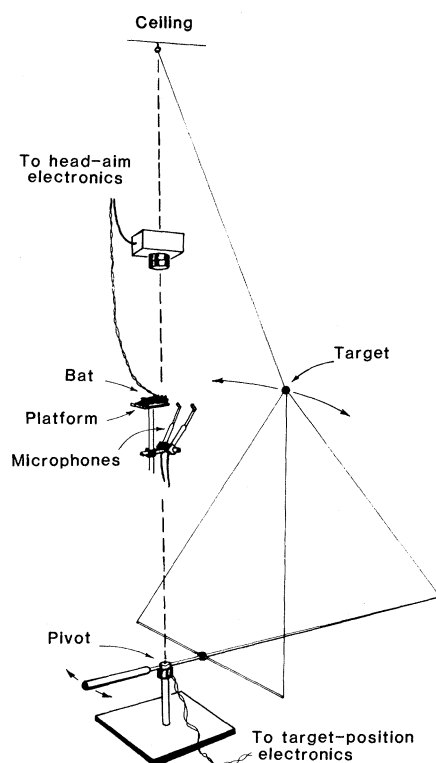


Fig. 1. Apparatus and procedure for studying target tracking by bats. The bat was trained to sit on the platform and keep its head aimed at a target (a black styrofoam ball 3.6 cm in diameter) suspended in space by four nylon monofilament lines (diameter 0.18 mm, and acoustically invisible to the bat) arranged tetragonally to keep the ball from swinging relative to the frame. These lines were attached to a T-shaped frame 1 m below the platform that could be moved by the experimenter to control the ball's position. To monitor the bat's head aim, light from two light-emitting diodes attached to the head was focused by a camera lens 60 cm above the bat onto a position-sensing diode (8). The lens and platform were mounted coaxially with the attachment point on the ceiling and the pivot of the T frame. Two microphones (9) placed slightly in front of and below the platform were used to record the bat's sonar emissions. A detector circuit converted the sounds to pulses, which were recorded on the tape recorder.

tracking strategies, we developed a new method for monitoring the bat's head aim. We have found that bats can track rapidly moving targets accurately and that they seem to do so with a nonpredictive strategy. The general assumption that bats in the field catch prey by predicting its position has not, to our knowledge, been demonstrated, and our laboratory results support the hitherto unconsidered possibility that they may use a nonpredictive strategy.

Two big brown bats (*Eptesicus fuscus*) were trained to sit on a platform and to track a small, spherical target being moved horizontally along an arc in space 42 cm away (Fig. 1). The angular position of the target, represented by the voltage from a potentiometer, was recorded on one track of a frequency modulated tape recorder. Head aim was determined from the position of two infrared light-emitting diodes mounted on the bat's head. The *x* and *y* coordinates of these diodes were read 100 times a second, under microprocessor control, with a two-axis, position-sensitive photodiode mounted above the bat. From these coordinates the microprocessor calculated the direction of the vector joining the diodes, which represents the azimuthal angle of the bat's head aim, and converted it to a voltage that was stored on the second channel of the tape recorder. Pulses marking the time of occurrence of

sonar emissions were recorded on the third channel (5). For analysis, head aim and target signals were low-pass filtered at 30 Hz and digitized in 2.55-second segments at 100 points per second.

An example of head-aim tracking is shown in Fig. 2, a and b. The bat was able to follow the target over a wide angular range even when the target's angular velocity was high (Fig. 2c). Tracking accuracy was measured by subtracting the target signal (Fig. 2b) from the head-aim signal (Fig. 2a) to yield the tracking error (Fig. 2d). The mean of the rectified error trace summarizes tracking accuracy for that 2.5-second sample. For 70 such samples from two bats (6), the average mean error was $4.7^\circ \pm 1.4^\circ$, that is, half the time the bat's head aim was within $\pm 4.7^\circ$ of the target's true position, which agrees well with the $\pm 5^\circ$ error measured from photographs (2). Linear regression of error against target velocity (Fig. 2, d and c) generally gave a highly significant correlation (mean $r = -0.73 \pm 0.09$), which suggests that the error at a given moment depends largely on target velocity. This is to be expected if the bat tracks by aiming at the target's last-known position (nonpredictive tracking), since the greater the target velocity, the farther it will have moved in the interval between sonar pulses.

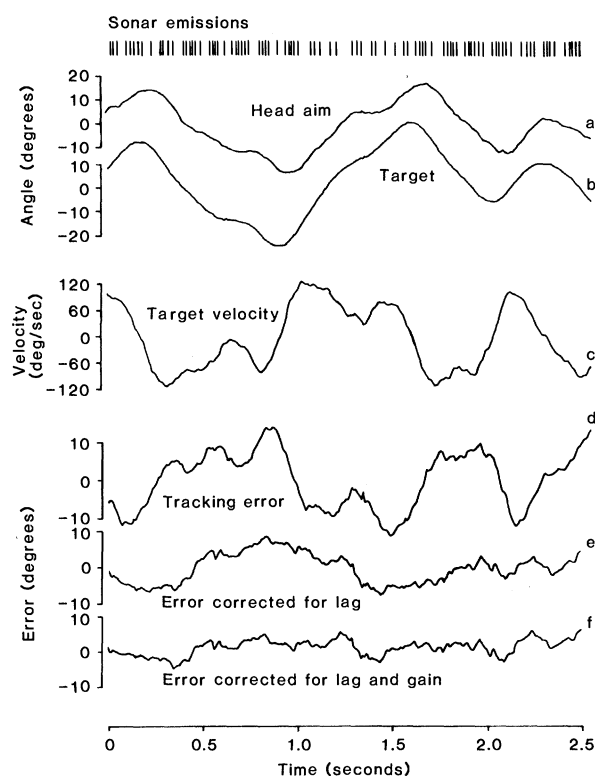
Another way of determining whether

predictive or nonpredictive tracking is being used is to compare the lag between head-aim and target position. Nonpredictive tracking must always entail a lag since the target will have moved while the bat is determining where to point its head. The lag should be longer than the average interval between sonar emissions since it includes the bat's signal processing and reaction times. On the other hand, with an appropriate predictive strategy the lag could be shorter than the interemission interval. In our experiments the lag, estimated by cross-correlating the head aim and target signals, was 66 ± 22 msec for one bat and 98 ± 27 msec for the other, whereas the average intervals between sonar emissions were 46 ± 15 and 55 ± 8 msec, respectively. That the lag is longer than the interval between sonar emissions suggests a nonpredictive tracking strategy.

A further test of the nonpredictive tracking hypothesis is to compare the bat's head-aim signal with the signal we would expect on the basis of a nonpredictive strategy to see if the discrepancy between the two could reasonably be attributed to "noise" in the system, that is, to the bat's inability to determine the target direction precisely or to aim its head exactly. Such errors should be random with respect to target parameters. The uncorrected error of Fig. 2d is not random in this way, since it is correlated with target velocity. If the bat's strategy is actually "aim at the target position obtained from the last sonar emission," given the high rate of sonar emissions (top of Fig. 2), its head aim should mirror target position but be slightly delayed; that is, the expected tracking signal is simply the target signal shifted in time to account for lag. In Fig. 2, head aim lags the target by about 60 msec. Advancing it by this amount and again subtracting the target signal gives the error corrected for lag (Fig. 2e). The mean error corrected for lag from all samples was $2.3^\circ \pm 0.7^\circ$.

However, we found that the lag-corrected error was still not independent of target parameters. The correlation between this error and target velocity ($r = -0.18 \pm 0.19$) is smaller than the uncorrected error, but there remains a substantial correlation ($r = -0.59 \pm 0.27$) with target position, that is, between traces b and e in Fig. 2. The reason seems to be that the bats did not track with unity gain. When the target was off the midline, the bat tended not to turn quite far enough, which resulted in an error that was correlated with the target's angular displacement. Tracking

Fig. 2. Bat's head aim (a) as it tracked an irregularly moving target (b). Subtracting (b) from (a) gives the tracking error (d), which is related to target velocity (c) ($r = -0.76$ in this example). That the bat's head aim (a) lags target position (b) is indicated by the later occurrence of waveform features in (a). Cross-correlation of (a) and (b) shows that the bat's head aim lags the target by 60 msec in this example. Advancing the head-aim signal by this amount and again subtracting (b) gives the lag-corrected tracking error (e), which is not correlated with target velocity, but is correlated with target position ($r = -0.83$). Correcting head aim for nonunity gain [peak-to-peak ratio of (a) to (b) is 0.87 in this example], results in error trace (f), which is only slightly correlated with traces (b) and (c) ($r = -0.37$ and -0.32 , respectively). The mean error in trace (f) is 1.6° . The bars at the top of the figure indicate the times of occurrence of sonar sounds.



gain, estimated from the ratio of peak-to-peak amplitude of tracking to target waveforms, averaged 0.87 ± 0.10 . We also found that the gain for a given tracking trial was related to the correlation coefficient between error corrected for lag and target position ($r = 0.78$, d.f. = 68, $P < 0.001$), suggesting that a bat uses different gains at different times, although what determines its choice is not clear. If the tracking signal is adjusted to bring the gain to unity for that trial before subtracting the target signal, the mean error, now corrected for lag and gain (Fig. 2f), is reduced to $1.6^\circ \pm 0.4^\circ$. Small correlations between error and target position and velocity remain ($r = 0.13 \pm 0.20$ and $r = -0.20 \pm 0.22$, respectively), but they account for relatively little of the error signal's variance, suggesting that a nonpredictive tracking strategy is a reasonable interpretation of our data. The residual error of $\pm 1.6^\circ$ is comparable to the angular resolving ability of *Eptesicus* determined with stationary targets (3). It also indicates that bats can locate prey at least as precisely as other highly auditory hunters, such as owls (7), that rely on passive listening.

W. MITCH MASTERS
ANNE J. M. MOFFAT
JAMES A. SIMMONS

*Institute of Neuroscience,
University of Oregon, Eugene 97403*

References and Notes

1. D. R. Griffin, *Listening in the Dark* (Yale Univ. Press, New Haven, 1958; reprinted by Dover, New York, 1974); A. Novick, in *Biology of Bats*, W. A. Wimsatt, Ed. (Academic Press, New York, 1977), vol. 3, pp. 73-287; J. A. Simmons, M. B. Fenton, M. J. O'Farrell, *Science* 203, 16 (1979); J. A. Simmons and S. A. Kick, in *Behavioral Physiology and Neuroethology: Roots and Growing Points*, F. Huber and H. Markl, Eds. (Springer, New York, 1983), pp. 267-279.
2. F. A. Webster and O. G. Brazier, *Aerospace Medical Research Laboratories Technical Report AMRL-TR65-172* (1965); F. A. Webster, in *International Conference on Sensory Devices for the Blind* (St. Dunstan's, London, 1967), pp. 63-87.
3. J. A. Simmons et al., *J. Comp. Physiol.* 153, 321 (1983).
4. S. A. Kick and J. A. Simmons, *J. Neurosci.* 4, 2725 (1984).
5. Experiments were normally conducted under dim light, although some control experiments were done in total darkness: this did not change the bat's tracking accuracy. We also looked at the bats' response to the support frame with the ball removed. They were unable to follow, indicating that they were indeed tracking the intended target.
6. Of the measurements reported in this paper the two bats differed significantly from each other only in calling rate, head lag, and mean error. This last difference is a consequence of the difference in tracking lag.
7. E. I. Knudsen, G. G. Blasdel, M. Konishi, *J. Comp. Physiol.* 133, 1 (1979).
8. Silicon Detector Corporation type SD-386-22-21-251.
9. Bruel and Kjaer type 4135.
10. We thank D. Presti and F. Presti for comments on the manuscript and D. Kon for assistance. Supported by the National Science Foundation, System Development Foundation, and Whitehall Foundation grants to J.A.S. and an NIH postdoctoral fellowship to W.M.M.

5 November 1984; accepted 25 March 1985

Coral Community Reproductive Patterns: Red Sea Versus the Great Barrier Reef

Abstract. *In contrast to many corals of the Great Barrier Reef, Australia, which are synchronous multispecific spawners, the abundant coral species in the northern Red Sea, Israel, exhibit temporal reproductive isolation. Spawning dates of 12 of the 13 Red Sea species followed lunar periodicity and were consistent throughout 3 years of study. Spawning periods of all species occurred in different seasons, different months, or different lunar phases within the same month. The high abundance of the corals studied at Eilat may be due in part to the advantages gained through not having overlapping spawning periods and settlement times.*

Our understanding of coral sexual reproduction is limited, and few generalizations can be made about the physical or biological factors responsible for the observed reproductive patterns (1). In particular, population ecology (2) and community structure of scleractinian

corals is not well known. Until now, the reproduction of only one Red Sea stony coral (*Stylophora pistillata*) had been studied (3). We examined reproductive patterns of 13 ecologically important coral species (4) at Eilat (northern Gulf of Eilat, Red Sea). Major reproductive ac-

Table 1. Coral spawning dates at Eilat during 1981 and 1982. Data for 1980 is illustrated in Fig. 1. The lunar month is divided into eight phases similar to those described by Atoda (8): 1, new moon; 3, first quarter; 5, full moon; 7, last quarter; 2, 4, 6, and 8 indicate intermediate lunar phases.

1981		1982	
Spawning dates	Lunar phase	Spawning dates	Lunar phase
<i>Stylophora pistillata</i> *			
January-June		December-June	
<i>Seriatotheca caliendrum</i> *			
4-5 May	1†	21-23 May	1†
31 May-2 June	1†	17-19 June	1†
28 June-3 July	8-1	16-20 July	8-1
27 July-1 August	8-1	13-18 August	8-1
27 August-1 September	8-1	13-18 September	8-1
26 September-1 October	8-1	12-17 October	8-1
23-28 October	8-1	12-17 November	8-1
26-28 November	1†	13-15 December	1†
<i>Alveopora daedalea</i> *			
18-24 October	6-8	5-11 November	6-8
15-21 November	6-8	4-10 December	6-8
17-23 December	6-8	2-8 January	6-8
<i>Pocillopora verrucosa</i>			
1-2 July	1	19-20 July	1
31 July-1 August	1	19-20 August	1
<i>Galaxea fascicularis</i>			
21-24 July	6-7	6-9 August	6-7
19-22 August	6-7	4-7 September	6-7
<i>Goniastrea retiformis</i>			
24-27 July	7	9-12 August	7
<i>Platygyra lamellina</i>			
30 June-5 July	1-2	19-24 July	1-2
1-3 August	1†	19-21 August	1†
<i>Favia fava</i>			
21-26 June	6-7	9-14 July	6-7
20-22 July	6†	5-7 August	6†
<i>Astropora myriophthalma</i>			
16-18 July	5	3-5 August	5
15-17 August	5	1-3 September	5
<i>Acropora hyacinthus</i>			
9-11 July	3	26-28 July	3
<i>Acropora scandens</i>			
16-18 June	5	4-6 July	5
<i>Acropora humilis</i>			
24-26 May	7	12-14 June	7
<i>Acropora eurystoma</i>			
19-21 May	5	6-8 June	5

*Brooding species. †Sporadic spawning (10 to 20 percent of population).